ISSN 0281-2762

LRAP--137

ABB
ASEA BROWN BOVERI

Development of a Heterodyne Laser Interferometer for Very Small High Frequency Displacements Detection.

Diploma work

by

Peter Bårmann

for

Asea Brown Boveri

and

Lund Institute of Technology
Department of Atomic Physics.

Supervisor: Anders Sunesson

Lund Reports of atomic physics
LRAP 137

October 1992.

contents

1 Abstract.

A heterodyne laser interferometer with detection electronics has been developed for measuring very small amplitude high frequency vibrations. A laser beam from a HeNe-laser is focused and reflected on the vibrating surface and the generated phase shifts are after interference with a reference beam detected with a photo detector and evaluated in a demodulation system.
The set-up is a prototype and in chapter eight, techniques to improve the accuracy and sensitivity of the system are presented. The present system can detect vibration amplitudes from around 1Å and is linear up to 250Å (± 4%). Frequencies from a few tens of kHz up to tens of MHz are covered. The low frequency region can be greatly improved by techniques described in Ch. eight. The minimum detectable displacement may be improved by narrowing the bandwidth of the detection system to the region of interest.

2 Introduction.

The traditional way to measure ultrasonic acoustic waves in solids is with piezoelectric transducers. The method described in this diploma work, the "vibrometer", has some advantages that can be very valuable for the user. At 10 MHz the ultrasound has a wavelength around 1 mm and that is a lot less than the ordinary piezoelectric transducer dimension at about 10 mm. Therefore the transducer signal will be very dependent of the incidence direction of the wave. The mass of the transducer acting as an impedance might also distort the result. A focused laser beam has none of these disadvantages as it has no impedance and can be focused to a spot in the micrometer range.
Another advantage with an optical probe is that it can easily be moved over the surface and it is possible to have a scanning probe-beam to produce a two-dimensional vibration picture.
A Michelson interferometer can be used to measure vibrations. However, it has to be slightly modified to become practical for vibration measurement use. The problem is the spurious phase variations induced by changes in optical path and in laser frequency.
There are different ways to solve this:
stabilised homodyne interferometry compensates the variations by actively moving one of the mirrors and thus the optical path;
heterodyne interferometry where one of the laser beams is given a slightly different frequency;
two-frequency interferometry, a combination of the other two.
For example see Ref. 1-5.

For high frequency and transient analyses the heterodyne method was chosen for this work.

3.1 Elementary interferometry.

Interferometry is based on the wave qualities of light; it can be described as electromagnetic waves and the waves may be superposed. The latter means that two waves meeting in a point in space will result in a wave with an amplitude equalling the sum of the amplitudes of the two waves (see Fig. 2). Amplitude in this case is the electromagnetic field vector but the same is true e.g. for waves in the sea and sound pressure waves in the air.

To achieve interference we need two overlapping light beams originating from the same source, producing coherent light. Coherent means that the electromagnetic fields oscillate with a constant phase difference. We can achieve this by splitting up a laser beam in two and then bring them together in one point.

Albert A. Michelson's interferometer from the late 19'th century describes the principle:

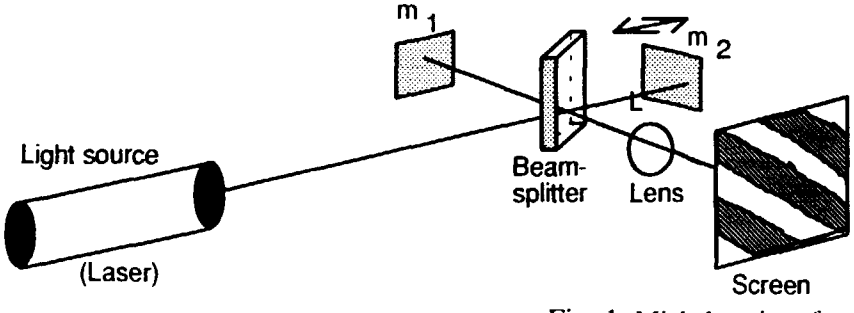

Fig. 1. Michelson interferometer.

The light beam is split in two beams in a beam-splitter (BS) and they hit the two mirrors m_1, m_2. The beam-splitter could e.g. be a glass plate which reflects a portion of the incident light and transmits the rest of it. On the mirrors the beams are reflected back to the BS where they overlap. A portion of each beam will now proceed collinear through the lens and to the view-screen where an interference pattern occurs. If mirror m_2 is displaced, the length L will be changed and thus the distance for that light beam to travel. This leads to a change in the phase relation between the light-waves on the screen. Mirror m_2 can be adjusted so that either light (beams in phase), darkness (beams out of phase) or something in between is seen on the screen.

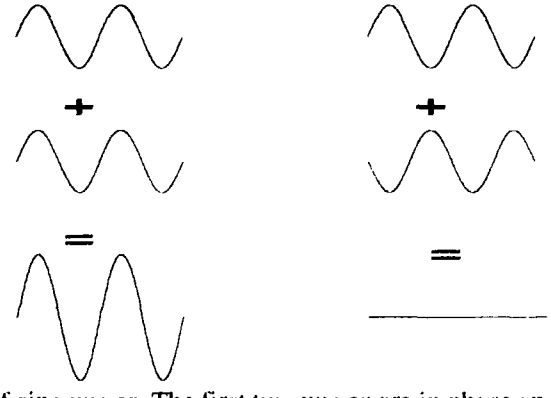

Fig 2. Superposition of sine waves. The first two waves are in phase and the result is a wave with twice the amplitude. The other two are out of phase and the result is zero.

To measure vibrations, we now let the light fall on a photo detector instead of on the screen. The detector produces an electric current proportional to the intensity of the received light. The current is viewed on an oscilloscope. The mirror m2 may be forced to vibrate by a piezo element, a material that expands and shrinks when an alternating voltage is applied.
The result from an experiment with the above described set-up is seen in Fig 3.

Homodyne Michelson interferometer.

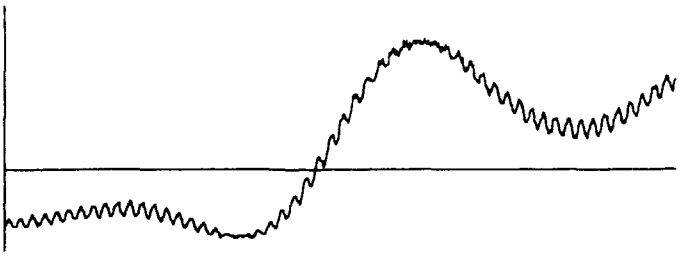

Fig. 3. Vibration measured with a Michelson interferometer. The small signal is a 5 kHz 15nm vibration from a piezo-electric transducer, the slow variations are changes in optical path in the interferometer arms due to background vibrations and temperature fluctuations.

Mathematically the electric field for the signal beam E_s, and the reference beam E_r, are described as:

$$E_s = A_s \exp i(2\pi\nu_L t + \varphi(t)) \quad (1)$$

$$E_r = A_r \exp i(2\pi\nu_L t - \theta) \quad (2)$$

where $\varphi(t)$ is the phase variation induced by the vibrating mirror and θ is the phase difference between the waves when $\varphi(t)=0$.

ν_L is the laser frequency and A_s and A_r are constants.
We now superpose the waves and get the irradiation

$$I = (E_s + E_r)(E_s + E_r)^* = |E_s|^2 + |E_r|^2 + E_s E_r^* + E_r E_s^* =$$

$$A_s^2 + A_r^2 + A_s A_r \exp i(2\pi\nu_L t + \varphi(t) - 2\pi\nu_L t + \theta) + A_s A_r \exp i(2\pi\nu_L t - \theta - 2\pi\nu_L t - \varphi(t)) =$$

$$A_s^2 + A_r^2 + A_s A_r \exp i(\varphi(t) + \theta) + A_s A_r \exp i(-\theta - \varphi(t)) =$$

$$A_s^2 + A_r^2 + 2A_s A_r \cos(\varphi(t) + \theta) \quad (3)$$

If we assume that the two waves have equal amplitude the signal varies between 0 and $4A^2$. We see that our vibration signal $\varphi(t)$ is superposed θ which is a slow phase variation induced by environmental factors.

This method is called homodyne interferometry; the two laser beams have the same frequency.

3.2 Heterodyne interferometry

With the homodyne technique two complications arise:

1 The signal is proportional to $\cos(\varphi(t)+\theta)$ and not directly to $\varphi(t)$. $\varphi(t)$ can be a very small phase change as a result of a small vibration amplitude. θ has its origin in fluctuations either in optical path (random spurious vibrations, pressure and temperature fluctuations) or in laser wavelength variations (interference beats or mode deviations, instability of laser cavity). It varies between 0 and π. The output-signal is then strongly dependent of θ which is not desirable. When θ is close to $\pi/2$ then a change in $\varphi(t)$ will make a considerable change in the signal, this is called the quadrature point, but if θ is close to 0 or π then the same change in $\varphi(t)$ will only have a minor effect, see Fig 4.

2 To get the detection electronics to lock on the signal we are limited to periodic mirror movements which is not desirable.

These two problems may be solved by having a small frequency difference between the two beams. This is heterodyne detection and is achieved by introducing an Acousto-Optic Modulator (AOM) (see appendix A) in the set-up. Letting the laser beam go through the AOM a part of it will be deflected and receive a frequency shift equalling the acoustic frequency in the AOM, while the rest of it will pass unaffected, both in direction and in frequency. As a result of the deflection no beam splitter is needed to divide the beam in two. The two light waves falling on the detector now have different frequencies and the detector produces a beat signal, with the AOM-frequency, superposed the vibration signal. We get a frequency modulated (FM) signal where the carrier frequency is the AOM-frequency and the modulations are the optical phase shifts from the displacement ($\varphi(t)$) and environmental changes (θ). A demodulation system may now lock on the beat signal. In the demodulation it is also possible to filter out the variation θ. In the set-up presented in this work the θ-variation is not extracted from the signal but in Ch. eight a method how to do so is described. In the set-up here presented the complication with the θ variation is partly bypassed by trigging on the signal when $\theta=\pi/2$ The trigged signal becomes : $\cos(\varphi(t)+\pi/2)\cong \varphi(t)$, (if $\varphi(t)$ is small); and we get a linear dependence between the displacement and the output signal.

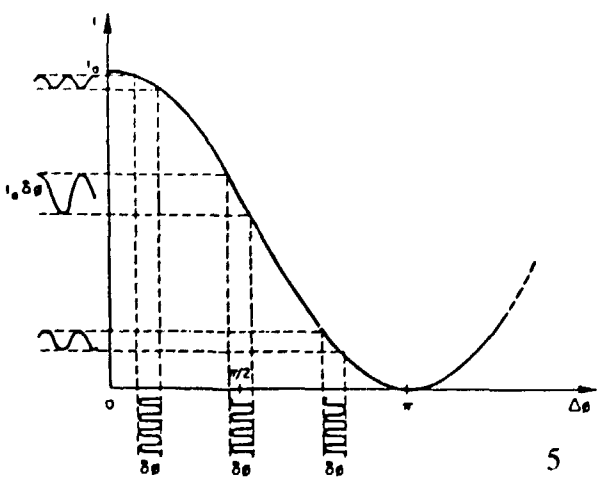

Fig. 4. The quadrature point in the fig. is when $\Delta\phi$ is close to $\pi/2$. At the quadrature point the output signal caused by $\delta\phi$ is large. When $\Delta\phi$ is close to 0 or π the output signal is small. [from 4]. In the text, θ corresponds to $\Delta\phi$ and φ to the variation $\delta\phi$.

4 Set-up and Description of function.

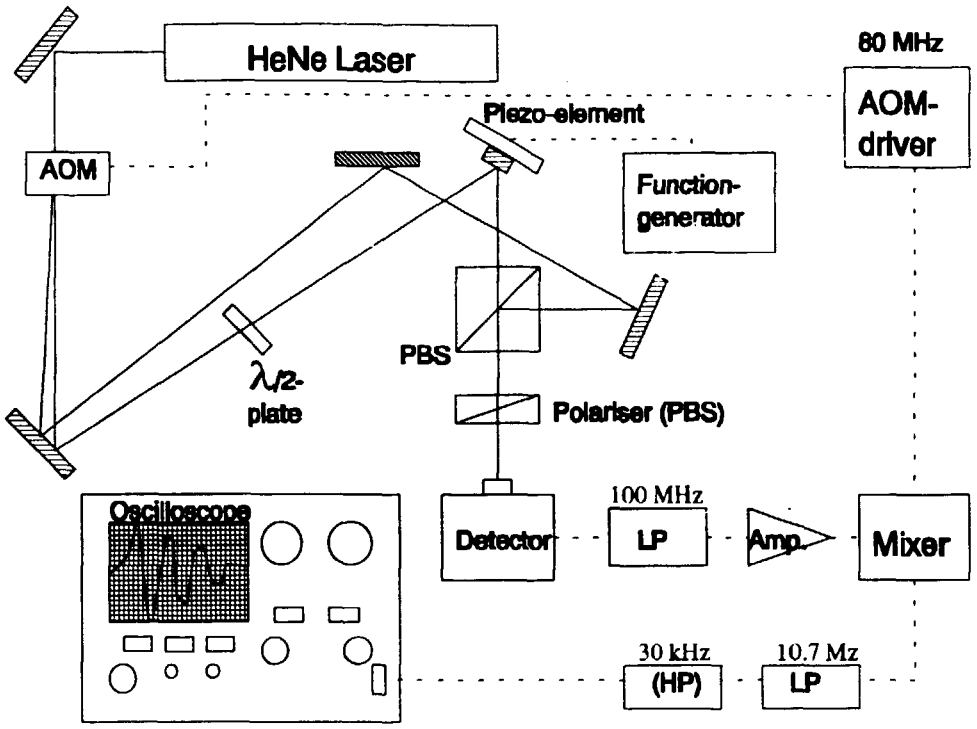

Fig. 5. The set-up for the vibrometer system.

The main components in the system are:

2,5 mW polarised HeNe laser (Saven),
Acousto-Optic Modulator (Isomet 1205C-2)
AOM-driver (Isomet D301B)
Fast photo detector (Electro-Optics Technology ET2010)
Low noise amplifier, 30 dB (Tron-Tech)
Mixer (Mini-Circuits ZFM3)
Digital oscilloscope (Tektronix 2431L)
Optical parts optimised for 632,8 nm.

The set-up is shown in Fig. 5. In this system a non stabilised, multimode and polarised laser is used. In the AOM the polarised laser beam is split up in one reference and one probe-beam. The probe beam has the laser frequency ν_L, and the reference beam the frequency ν_L+f, where f=80 MHz is the AOM acoustic frequency. The reference beam is reflected into the polarising beam-splitter (PBS) where it is further reflected, since it is horizontally polarised, towards the detector. The probe-beam first passes through a half-wave plate were it becomes horizontally polarised before it is reflected on the piezo element. It then passes through the PBS because of the polarisation and proceeds collinearly with the reference beam through a polariser (a PBS) onto the detector.

The two beams are perpendicularly polarised so no interference can be detected before the polariser. The polariser is oriented in the bisector to the beams, and the polarisation components in this direction will interfere. By using the polarisation states in this way the light effect falling on the detector area is maximised: almost 100 % reflection or transmission, depending on polarisation, is achieved in the first polarising beam-splitter, so the beams entering the polariser have close to half the laser output power each. The received power in the detector is :

$$P_d \approx \frac{1}{2}P_L\frac{1}{\sqrt{2}}+\frac{1}{2}P_L\frac{1}{\sqrt{2}}=\frac{1}{\sqrt{2}}P_L \approx 0.71P_L$$ (P_L=laser power; P_d=received detector effect).

To demodulate the beat signal from the detector it is mixed with the AOM-driver's 80 MHz signal. Before the mixing the signal is amplified by a low noise amplifier. The result from the mixing is recorded on a digital oscilloscope. The 100 MHz low-pass-filter after the detector stops high frequency disturbances, such as mode beats from the laser, to affect the mixing; and the 10.7 MHz low-pass-filter after the mixer only lets the low-frequency vibration phase shifts through.
High-pass-filtering the mixed signal suppresses the low-frequency spurious vibrations and phase shifts caused by pressure and temperature fluctuations and laser instability.
By varying the amplitude of the RF-signal from the AOM-driver the intensity distribution between the two output beams are controlled.

5. Signal detection.

5.1 Modulation.

The two beams falling on the detector are described as

$$E_s = \sqrt{P_s}\exp i(2\pi \nu_L t + \Delta\psi(t)) \tag{4}$$

$$E_r = \sqrt{P_r}\exp i\left(2\pi(\nu_L t - f_{ao})t\right). \tag{5}$$

They are equally polarised, spatially and temporally coherent. The reference beam E_r is frequency modulated with f_{ao} from the AOM. E_s, the signal beam, is phase modulated by the piezo elements movements. P_s and P_r are the optical powers from the beams. The phase difference $\Delta\psi(t)$ consists of two terms; $\Delta\theta$, the environment-induced phase-difference between the waves and $\Delta\varphi(t)$, the phase shift caused by the vibrations of the piezo surface. For $\Delta\varphi$ we have (see Fig. 6):

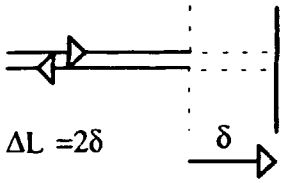

Fig. 6. Mirror displacement vs. change in optical path.

$$\Delta\varphi = -\Delta L\frac{2\pi}{\lambda} = -2\delta\frac{2\pi}{\lambda} = -\frac{4\pi}{\lambda}\delta.$$

Thus

$$\Delta\psi(t) = \Delta\theta + \Delta\varphi(t) \qquad \text{where} \tag{6}$$

$$\Delta\varphi(t) = -\frac{4\pi}{\lambda}\delta(t). \tag{7}$$

If the incidence of the signal beam is not perpendicular to the vibrating object, say by the angle α, $\delta(t)$ is modified to: $\Delta\varphi(t) = -\dfrac{4\pi}{\lambda\cos(\alpha)}\delta(t).$ (8)

The two interfering waves give the total power on the detector surface :

$$P_d(t) = (E_s + E_r)(E_s + E_r)^* = |E_s|^2 + |E_r|^2 + E_s E_r^* + E_r E_s^* \tag{9}$$

Because of not ideal conditions we cannot achieve total interference and a correction factor is necessary in the cross-terms:

$$P_d(t) = P_s + P_r + \beta\left(\sqrt{P_s P_r}\exp i(\Delta\psi(t) + 2\pi f_{ao}t) + \sqrt{P_s P_r}\exp i(-\Delta\psi(t) - 2\pi f_{ao}t)\right) =$$

$$= P_s + P_r + 2\beta\sqrt{P_s P_r}\cos(\Delta\psi(t) + 2\pi f_{ao}t) \tag{10}$$

The efficiency factor β origins from misalignments among the optical components and an unstable and not strictly monochromatic laser source.

To convert the above expression to the photo current generated by the absorption of photons, we have

$$I_r = \eta e \frac{P_r}{h\nu_L} \quad \text{and} \quad I_s = \eta e \frac{P_s}{h(\nu_L + f_{ao})} \approx \eta e \frac{P_s}{h\nu_L} \quad (f_{ao} << \nu_L) \tag{11}$$

η is the quantum efficiency of the photo detector, e is the electron charge and h is Planck's constant.
Thus the photo current:

$$I(t) = \frac{\eta e}{h\nu_L} P_d(t) = I_s + I_r + 2\beta\sqrt{I_s I_r}\cos\left[2\pi f_{ao} t + \Delta\psi(t)\right]. \tag{12}$$

The alternating component can be written, given (6):

$$I_{ac}(t) = 2\beta\sqrt{I_s I_r}\cos\left[2\pi f_{ao} t + \Delta\theta + \varphi(t)\right] \tag{13}$$

and we get a frequency modulated (FM) signal with three components: the AOM modulation frequency (f_{ao}), environment phase-shift (θ) (change in optical path and laser frequency) and displacement phase-shift ($\varphi(t)$). (13) has to be demodulated to get a signal proportional to the displacement (see Ch. 5.2). In a demodulation system the AOM frequency is the carrier frequency and the modulations are the optical phase shifts from the displacement and environmental changes.

If we expand the cosine factor we get

$$2\beta\sqrt{I_s I_r}\left[\cos(2\pi f_{ao} t + \Delta\theta)\cos(\varphi(t)) + \sin(2\pi f_{ao} t + \Delta\theta)\sin(\varphi(t))\right]. \tag{14}$$

If the displacement is very small we can approximate :

$$\varphi(t) \ll \pi \Rightarrow \sin(\varphi(t)) \approx \varphi(t) \text{ and } \cos(\varphi(t)) \approx 1$$

and using (7) :

$$I_{ac} = 2\beta\sqrt{I_s I_r}\left[\cos(2\pi f_{ao} t + \Delta\theta) \times 1 - \sin(2\pi f_{ao} t + \Delta\theta) \times \frac{4\pi}{\lambda}\delta(t)\right]. \tag{15}$$

The alternating photo current is, at a certain value for $[2\pi f_{ao} t + \Delta\theta]$, approximately linearly dependent of the displacement. If the phase shift caused by the vibrating object stays within 0.5 radians the approximation error due to the linearisation is less than 4%. 0.5 radians corresponds to $0.5/4\pi \times 6328$ Å$\approx$ 250 Å, which could be used as an upper displacement limit for this technique.

When looking at transients we should express the displacement as a Fourier series. These transients may have a wide spectrum of frequencies which extend over tens of megahertz and amplitudes very small compared to the laser wavelength. We write

$$\delta(t) = \sum_{n=0}^{\infty} d_n \cos(2\pi n f_0 t + \varphi_n) \tag{16}$$

where f_0 is the fundamental frequency of the movement, d_n and φ_n represent the amplitudes and phases of the spectral components.
The phase variation is then expressed as:

$$\Delta\varphi(t) = -\frac{4\pi}{\lambda}\delta(t) = -\frac{4\pi}{\lambda}\sum_{n=0}^{\infty} d_n \cos(2\pi n f_0 t + \varphi_n). \tag{17}$$

I_{ac} thus becomes, using the same linearisation as above:

$$I_{ac} = 2\beta\sqrt{I_s I_r}\left[\cos(2\pi f_{ao} t + \Delta\theta)\times 1 + \sin(2\pi f_{ao} t + \Delta\theta)\times\Delta\varphi\right] =$$

$$2\beta\sqrt{I_s I_r}\left[\cos(2\pi f_{ao} t + \Delta\theta) - \sin(2\pi f_{ao} t + \Delta\theta)\times\frac{4\pi}{\lambda}\sum_{n=0}^{\infty} d_n \cos(2\pi n f_0 t + \varphi_n)\right] =$$

$$2\beta\sqrt{I_s I_r}\left[\cos(2\pi f_{ao} t + \Delta\theta) - \frac{4\pi}{\lambda}\sum_{n=0}^{\infty} d_n \sin(2\pi f_{ao} t + \Delta\theta)\times\cos(2\pi n f_0 t + \varphi_n)\right] =$$

$$2\beta\sqrt{I_s I_r}\left[\cos(2\pi f_{ao} t + \Delta\theta) - \frac{2\pi}{\lambda}\sum_{n=0}^{\infty} d_n\left\{\sin(2\pi(f_{ao} + n f_0)t + \Delta\theta + \varphi_n) + \sin(2\pi(f_{ao} - n f_0)t + \Delta\theta - \varphi_n)\right\}\right]. \tag{18}$$

We see that the first term is the frequency carrier (f_{ao}), with an amplitude proportional to the product of the optical outputs of the two interfering waves. The second term contains all the frequency components of the displacement, as side bands to the frequency carrier. The amplitude of each of these is proportional to the displacement amplitude at the corresponding frequency. In these components we also have the low frequency spurious fluctuations of the signal caused by environmental factors and laser instability. The frequency carrier and the side-bands are seen in Fig. 7.

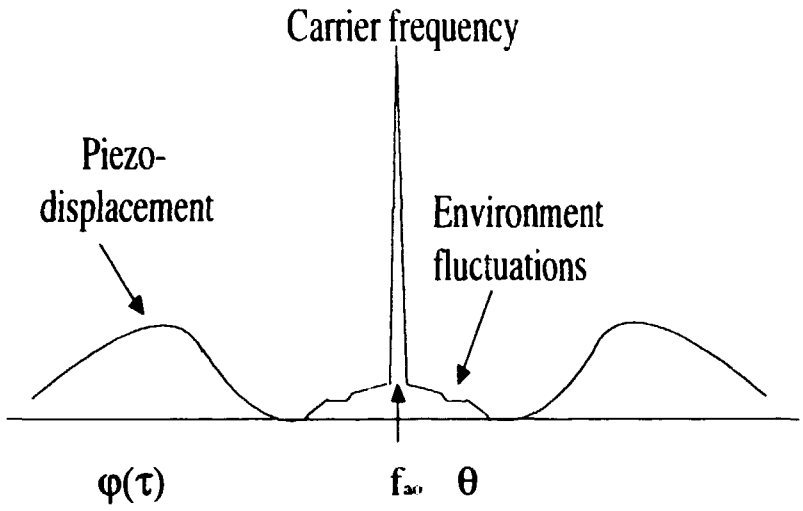

Fig. 7. Spectrum of detector signal with the carrier frequency f_{ao} and the sidebands from the displacements, φ, and slow variations, θ.

5.2 Demodulation.

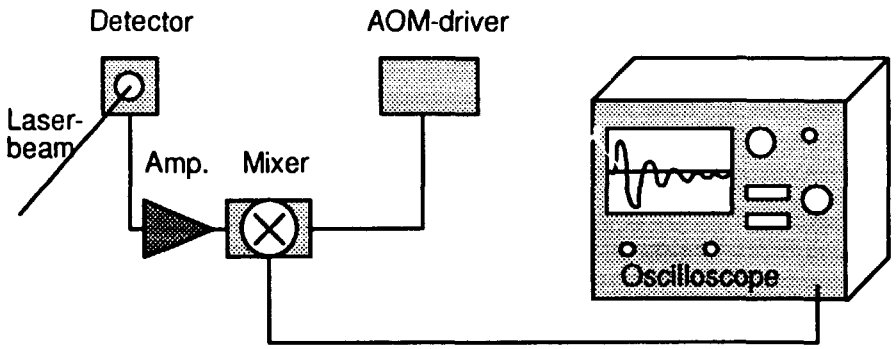

Fig. 8 Demodulation system.

There are different possible methods to retrieve the interesting signal, the displacement of the object. The one chosen in this work is to mix the detector signal with the AOM-frequency, and the mixer output is proportional to the phase shifts of the light waves. This signal may e.g. be recorded by an oscilloscope or a transient recorder.

5.2.1 The mixer.

A mixer is a simple electronic circuit multiplying the two incoming signals, resulting in the sum and difference frequencies. Say we have two harmonic waves x(t) and y(t), differing approximately $\pi/2$ in phase. The result becomes :

$$\begin{aligned} z(t) &= Kx(t)y(t) = KA\sin(2\pi f_x t+\theta_x)B\cos(2\pi f_y t+\theta_y) = \\ &\frac{KAB}{2}\left\{\sin\left[2\pi f_x t+\theta_x+2\pi f_y t+\theta_y\right]+\sin\left[2\pi f_x t-\theta_x-2\pi f_y t-\theta_y\right]\right\} = \\ &\frac{KAB}{2}\left\{\sin\left[(2\pi f_x+2\pi f_y)t+\theta_x+\theta_y\right]+\sin\left[(2\pi f_x-2\pi f_y)t+\theta_x-\theta_y\right]\right\} \end{aligned} \tag{19}$$

K is just a multiplication factor. If $f_x = f_y = f$ we'll receive one low-frequency and one high frequency term :

$$z(t) = \frac{KAB}{2}\left\{\sin(4\pi ft+\theta_x+\theta_y)+\sin(\theta_x-\theta_y)\right\} \tag{20}$$

Low-pass filtered we get :

$$z(t) = \frac{KAB}{2}\sin(\theta_x-\theta_y) \tag{21}$$

the phase difference of the two input signals.

5.2.2 Retrieving the vibration signal.

Before mixing, the detector signal is filtered and amplified. The 100 MHz low-pass-filter stops high frequency mode beating disturbance from the laser to affect the mixing. The laser runs in multiple mode with a mode-spacing of 400 MHz and two interfering modes will give a beat frequency of 400 MHz. The amplification is set to maximise the conversion in the mixer. The dc-component in the detector signal is here disregarded. It is filtered out in the low pass filtering (Eq. 25).
The two input signals to the mixer expressed in voltage are (from Eq. 15; U=RI) :

$$U_{ac}(t) = 2\beta\sqrt{U_s U_r}\left[\cos(2\pi f_{ao}t + \Delta\theta) + \sin(2\pi f_{ao}t + \Delta\theta)\times\Delta\varphi(t)\right] \tag{22}$$

where $\Delta\varphi(t) = -\frac{4\pi}{\lambda_L}\delta(t)$ as before and

$$U_{ao}(t) = A\sin(2\pi f_{ao}t). \tag{23}$$

Say for simplicity that $A = \sqrt{U_s U_r}$.

The power $P_m(t)$ of the mixed signal (R_m is the resistance in the mixer) :

$$P_m(t) = \frac{U_{ac}\times U_{ao}}{R_m} =$$

$$2\beta\frac{U_s U_r}{R_m}\left[\cos(2\pi f_{ao}t + \Delta\theta)\sin(2\pi f_{ao}t) + \sin(2\pi f_{ao}t + \Delta\theta)\sin(2\pi f_{ao}t)\times\Delta\varphi(t)\right] =$$

$$2\beta\frac{U_s U_r}{R_m}\left\{\left[\frac{1}{2}\sin(2\pi f_{ao}t + 2\pi f_{ao}t + \Delta\theta) + \frac{1}{2}\sin(2\pi f_{ao}t - 2\pi f_{ao}t - \Delta\theta)\right] + \right.$$

$$\left. + \left[\frac{1}{2}\cos(2\pi f_{ao}t + 2\pi f_{ao}t + \Delta\theta) - \frac{1}{2}\cos(2\pi f_{ao}t - 2\pi f_{ao}t - \Delta\theta)\right]\Delta\varphi(t)\right\} =$$

$$\beta\frac{U_s U_r}{R_m}\left\{\sin(2\pi 2 f_{ao}t + \Delta\theta) + \left[\cos(2\pi 2 f_{ao}t + \Delta\theta)\right]\Delta\varphi(t) + \sin(-\Delta\theta) - \left[\cos(-\Delta\theta)\right]\Delta\varphi(t)\right\}. \tag{24}$$

Low-pass filter this to get rid of modulation signal :

$$P_{mLP} = -\beta\frac{U_s U_r}{R_m}\left\{\sin(\Delta\theta) + \cos(\Delta\theta)\Delta\varphi(t)\right\}. \tag{25}$$

If P_m is trigged when $\Delta\theta = 0$ we get

$$P_{mLP} = -\beta\frac{U_s U_r}{R_m}\left\{\sin(0) + \cos(0)\Delta\varphi(t)\right\} = -\beta\frac{U_s U_r}{R_m}\Delta\varphi(t) \tag{26}$$

and we finally arrive at :

$$P_{mLP} = \beta \frac{U_s U_r}{R_m} \frac{4\pi}{\lambda_L} \delta(t) \quad = K \frac{4\pi}{\lambda_L} \delta(t) \tag{27}$$

which is the displacement multiplied by a constant factor, $K \cdot 4\pi/\lambda_L$.
For the evaluation when the displacement is expressed as a Fourier series, see appendixB.

5.2.3 Calibration and evaluating the vibration signal.

In (25) we see that the signal fluctuates between ±K. Since the displacement is small, the term $\sin(\Delta\theta)$ will be the dominant one and the vibration signal will only be a small ripple on the $\sin(\Delta\theta)$-term fluctuating between ±K. In Fig. 9 the total signal (25) is seen.
The figure shows the phase shifts from environmental variations in optical path and laser frequency. The mirror displacement of a few tenths of Angstrom is to small to be clearly seen in the figure. To see the vibration signal we have to enhance the sensitivity on the oscilloscope as in Fig. 10. To calculate the displacement of the mirror in meters out of equation (27), we divide the signal by $K \cdot 4\pi/\lambda$.
In practice we first measure the total variation ±K, as in Fig. 9. This will be the calibration of the system. K multiplied by $4\pi/\lambda_L$, λ_L is the laser wavelength, is the calibration factor we divide the signal (in Fig. 10) by to get the displacement in meters.

So the formula for the displacement of the vibrating surface is, if we call ±K, the total span of the signal; U_{span}:

$$\delta(t) \quad = \frac{U_{displ.}}{K} \frac{\lambda_L}{4\pi} \text{[m]} = \quad \frac{U_{displ.}}{U_{span}} \frac{\lambda_L}{2\pi} \text{[m]} \tag{28}$$

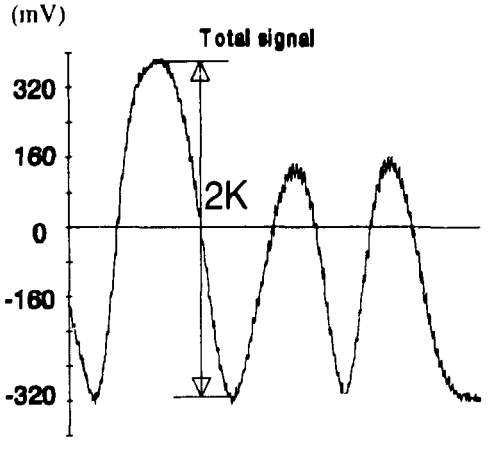

Fig. 9. Total signal with slow variation and Piezo vibration signal.

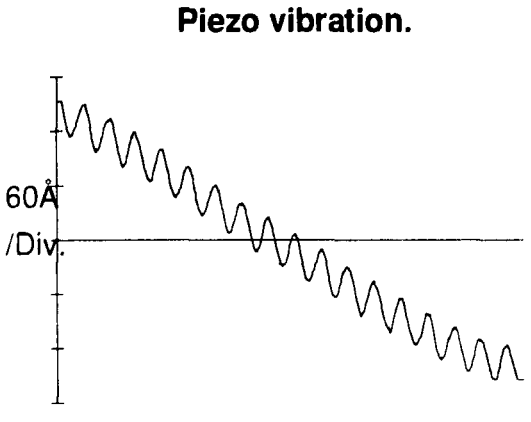

Fig. 10. Enhanced detail picture of vibration. Displacement is 50Å.

6 Test examples.

In this chapter some test examples recorded with the apparatus on a Tektronix 2431L digital oscilloscope are presented.

6.1 Harmonic displacements.

Fig. 11 shows the displacement when the piezo-electric transducer is driven by a harmonic 1 MHz, 4V signal.

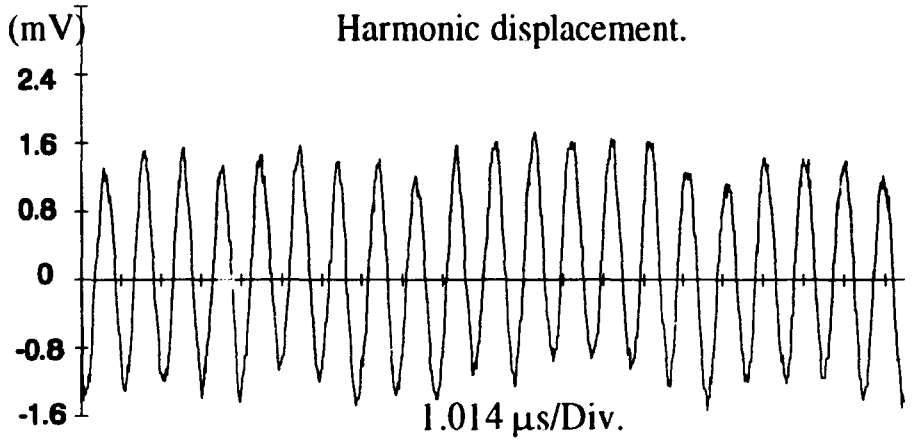

Fig. 11. Harmonic Piezo displacement.

In fig. 11 above the total voltage span (2K in fig. 9) of the signal was 435mV. The Piezo signal voltage is 3.5·0.8mV=2.8mV. With these values equation 28 gives us the displacement :

$$\delta(t) = \frac{U_{displ.}}{U_{span}} \frac{\lambda_L}{2\pi} [\mathrm{m}] = \frac{2.8}{435} \cdot \frac{6328 \cdot 10^{-10}}{2\pi} [m] = 6.48 \cdot 10^{-10} [m] \approx 6.5 \mathring{A}.$$

The frequency is calculated to :

$$f = \frac{16}{16.5 \cdot 1.014 \cdot 10^{-6}} s^{-1} = 0.96 MHz.$$

The characteristics for the Piezo-electric transducer is specified to 2Å/V and with a 4V Piezo voltage we would expect 8Å instead of the found 6.5Å. The discrepancy should, because of the physical nature of the interferometer result, be due to a uncertainty in the transducer specification.

In fig. 11 a weak signal at around 100 kHz can be discerned, superposed the 1 MHz signal. This is probably electronic noise; pickup in cables, produced in amplifier, filter or mixer.

6.2 Transients.

A Tektronix pulse generator is used to produce square-wave pulses to excite the piezo-electric transducer. Maximum output voltage from the generator is 30V and is fed directly to the piezo element.

1 A 30V 500 ns square pulse.

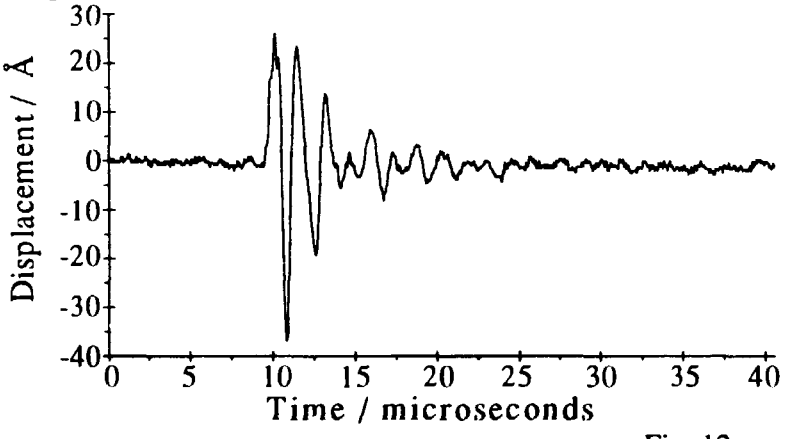

Fig. 12.

We see the piezo-electric transducer ringing at 0.74 MHz and maximum displacement 63 Å pp. The exciting pulse is inserted in the figure. The noise is less than 2 Å, peak to peak (pp).

2 A 30V 500 ns square wave pulse, averaged over 32 pulses.

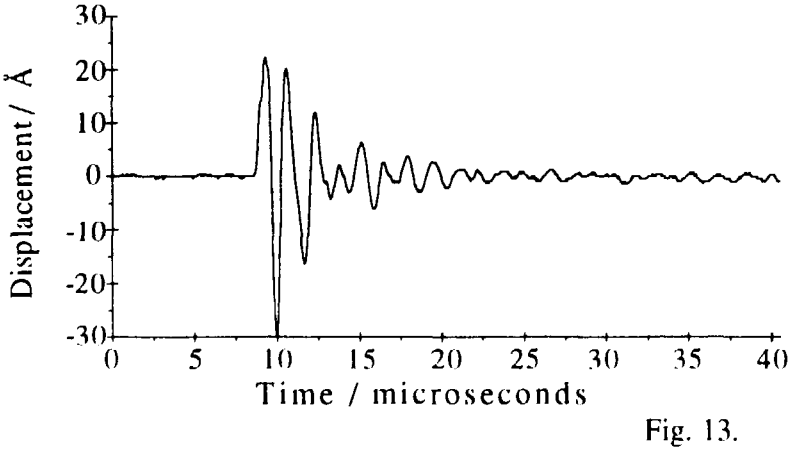

Fig. 13.

The cell rings at 0.74 MHz and, not surprisingly, the averaging process decreases the measured maximum displacement slightly to 54 Å pp. The signal resolution is limited by the digitising noise in the oscilloscope which is approximately 0.8 Å pp.
The pictures are almost identical except for the lower noise level after averaging. The conclusion of this is that the piezo element has a significant and repetitive pulse response and that the measuring method is very precise.

3 A 5V 500 ns square wave pulse.

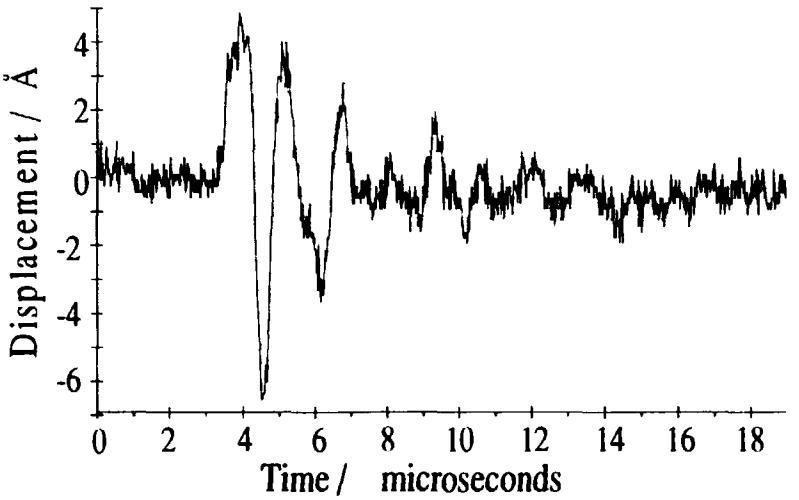

Fig. 14.

Here the voltage is lowered to get a more noise-distorted picture. The noise corresponds to 1 Å pp. and the signal is still clearly detectable when the maximum displacement is 11 Å pp. The frequency is also found here to be 0.74 MHz.

4 A 30V 22 us square wave pulse.

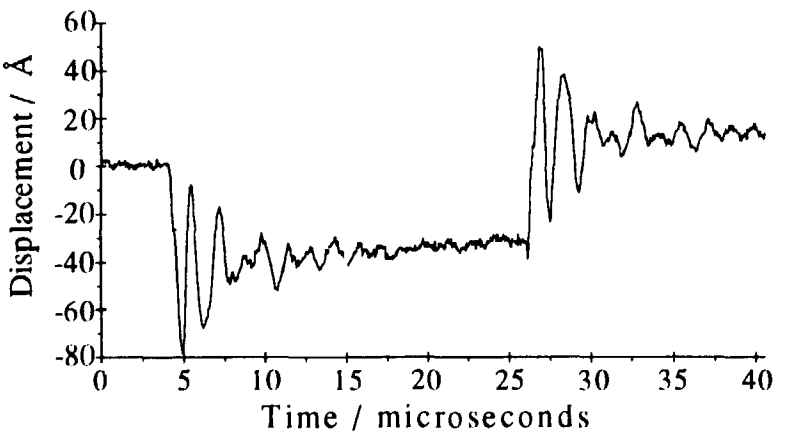

Fig. 15.

With the pulse 22 us wide we get step function responses instead of pulse response. The maximum displacement is 67 Å pp, about the same as before, and the element rings as expected at 0.74 MHz. We can also see the "static" displacement of 43 Å after extrapolating and correcting the signal for the slight inclination. The digitising noise is 2 Å pp.

7 Sensitivity analysis - noise.

7.1 Theoretical limit.

The sensitivity of the apparatus is limited by the noise in the output signal.
We shall now calculate the theoretical minimum detection level where it is assumed that it occurs when the signal to noise ratio equals 1 (Ref. 3). Since noise and a phase shift signal is converted in the same way in the mixer we can look at the S/N-ratio before the mixing without changing the final result after the mixing. Noise added in other components than the detector is here disregarded. For the noise level it is assumed that the so called 1/f-noise may be neglected because of the modulation frequency of 80 MHz. It is assumed that the noise only descends from the thermal noise, also called Johnson noise, and the shot-noise in the photo diode detector. The physical mechanisms behind the 1/f-noise are not well understood and no general theory for it is accepted but experimentally it has been found to be proportional to the detector current and approximately inversely proportional to the frequency, which leads us to the assumption above. The total noise current is then given by :

$$i_{noiseRMS} = \sqrt{i_{snRMS}^2 + i_{thRMS}^2} \tag{29}$$

where 'sn' stands for shot-noise, 'th' for thermal noise and 'RMS' for the root mean square value of the currents. The RMS-value of the shot-noise current is [Ref. 6] :

$$i_{snRMS} = \sqrt{2e(I_s + I_r)B}\,. \tag{30}$$

e is the electron charge, I_s and I_r the photo currents generated by signal and reference beam and B is the bandwidth for the detection system.
For the thermal noise we have [Ref. 10]:

$$i_{thRMS} = \sqrt{4k\frac{T}{R_{eff}}B}\,. \tag{31}$$

In this equation k is the Boltzmann constant, T the absolute temperature and R_{eff} is the effective load resistance of the detector.
The signal photo current (Eq. 15) was :

$$I_{ac} = 2\beta\sqrt{I_s I_r}\left[\cos(2\pi f_{ac}t + \Delta\theta)\times 1 - \sin(2\pi f_{ac}t + \Delta\theta)\times\frac{4\pi}{\lambda}\delta(t)\right] \tag{32}$$

The first term is of no interest and is neglected. In the second term the high frequency part $2\pi f_{ac}t$ is stopped by the filter after the mixer and doesn't affect the level of our interferometer signal. If the signal is always read when $\sin(\Delta\theta) = 1$, the photo current of interest simplifies to :

$$I_{ac} = 2\beta\sqrt{I_s I_r}\,\frac{4\pi}{\lambda}\delta(t). \tag{33}$$

Let us assume that the displacement is a simple harmonic motion;

$$\delta(t) = \xi\cos(2\pi ft). \tag{34}$$

The RMS-value of the photo current thus becomes :

$$i_{acRMS} = \frac{1}{\sqrt{2}} 2\beta\sqrt{I_s I_r}\frac{4\pi}{\lambda}\xi \quad = \beta\sqrt{2I_s I_r}\frac{4\pi}{\lambda}\xi \tag{35}$$

where $\frac{1}{\sqrt{2}}$ is the RMS-value of $\cos(2\pi ft)$.

S/N=1 when $i_{acRMS} = i_{nRMS}$:

$$\beta\sqrt{2I_s I_r}\frac{4\pi}{\lambda}\xi_{min} = \sqrt{2e(I_s + I_r)B + 4k\frac{T}{R_{eff}}B} \tag{36}$$

$$\xi_{min} = \frac{\lambda\sqrt{B}}{4\pi\beta}\sqrt{\frac{e(I_s + I_r) + 2k\frac{T}{R_{eff}}}{I_s I_r}} \tag{37}$$

Consider an ideal situation where

$$\beta = 1 \text{ and } \quad I_s = I_r = \frac{\lambda\eta eP}{2hc} \tag{38}$$

λ is the laser frequency, η the quantum efficiency of the detector, P the laser power, h Planck' s constant and c is the speed of light.

We finally arrive at :

$$\xi_{min} = \frac{\sqrt{B}}{2\pi}\sqrt{\frac{hc\lambda}{\eta P} + \frac{2kTh^2c^2}{\eta^2 e^2 P^2 R_{eff}}}. \tag{39}$$

With our numerical values

B = 10.7 MHz, P = 1mW (for each beam), and say $\eta = 0.5$,

λ=6328 Å, T=293 Kelvin, R_{eff} =50 Ω

the minimum detectable amplitude for a harmonic mirror displacement is :

$$\xi_{min} = 0.18\text{Å}.$$

The thermal noise alone sets the limit at 0.16Å while only shot noise would set the limit at 0.08Å.

On a 1 Hz bandwidth we get :

$$\xi_{1Hz\,min} = 5.6\cdot 10^{-5}\,\text{Å}.$$

ξ_{min} is the amplitude for the harmonic vibration but the displacement peak to peak is twice as big. Thus, the minimum detectable displacement is :

Δ_{min}=0.36 Å.

The theoretical limit however is dependent of the variables λ, B, P, T and R_{ref}. A smaller bandwidth of the detection system will lower the thermal and shot-noise equally but will result in a smaller detectable frequency range. Since the thermal noise is the dominant one, the easiest way to lower the noise is either to cool the equipment, use higher laser power or have a higher effective load resistance for the detector. The latter alternative is probably the best and easiest. A current amplifier with high input impedance (if only a few times higher than our 50 Ω) after the detector would put the thermal noise below the shot noise, and the minimum detectable displacement would be 0.08 Å instead. To get even this level down, shorter laser wavelength or higher laser power is needed.

7.2 Noise measurements.

Since the noise level sets the limit for the sensitivity of the apparatus the main objective is to minimise the electronic noise and to come as close as possible to the theoretical values. Ways to minimise the electronic noise is to shorten signal paths and ground judiciously.
The noise is measured in two ways: direct measurement where the actual signal recorded on the oscilloscope is analysed (Ch. 7.2.1); and spectral noise analyses where the frequency components of the noise are measured with a lock-in amplifier (Ch. 7.2.2). In the first method all the frequencies can be measured at the same time and in the second method the amplitudes of the frequency components are used to calculate the equivalent total noise.

7.2.1 Direct measurement.

In Fig. 17 the noise is recorded without a vibration signal and with a detection bandwidth of 1 MHz, limited by an amplifier after the mixer. The RMS-value is approximated by the standard deviation formula:

$$\delta = \sqrt{\frac{n\sum x^2 - \left(\sum x\right)^2}{n^2}} \qquad (40)$$

and is evaluated with computer. The results are :

RMS noise: 0.46 mV corresponding to: 0.16 Å,
peak-peak noise: 2 mV ------"------ 0.7 Å.
1 Hz bandwidth noise: $1.6 \cdot 10^{-4}$ Å.

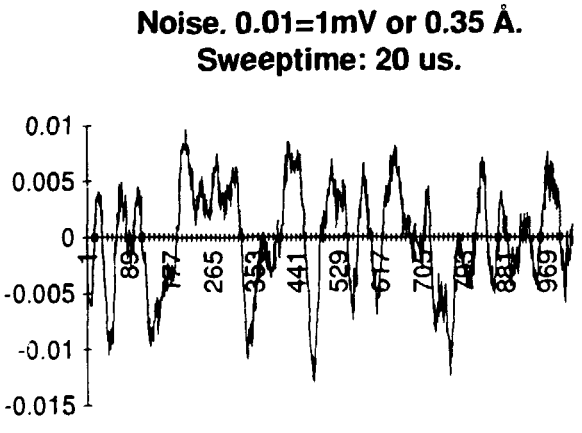

Fig. 16. Output noise.

The 1 Hz bandwidth noise level found here is about three times bigger than the theoretical values. However, the conditions for the theoretical and experimental results are different. Since the oscilloscope takes a picture of the noise over a finite time, frequencies with a period a few times longer than the time window will not show; the time window will act as a high-pass filter. If the sweep time is short only high

frequencies will be visible, and if it is long the total spectrum can be measured. A problem is that at lower frequencies the environment and laser instability-induced phase-shift signals will interfere in the noise measuring, which results in a practical, lowest frequency limit for the noise measurement. The total experimental noise is therefore really higher than here presented.

Depending on which frequency region we are interested in we may choose the width of the time window. By narrowing it, and thus lowering the band-width of the detection system, we may improve the minimum detectable displacement limit. This is clearly seen in Eq. 36; minimum detectable displacement is proportional to the square root of the bandwidth.

In Fig. 16 we can see that the noise is not really white, which thermal noise is supposed to be. It is probable that a great deal of the noise comes from the electric components and pickup in e.g. cables.

To experimentally determine if this seems credible the light intensity on the detector was damped to 10% of total power by a grey-filter. Since shot-noise is proportional to the square root of the light power (Eq. 27) and thermal noise is unaffected of it (Eq. 28) the noise should a fall to 30%, if it is shot-noise limited and not at all if the thermal noise is dominant. The result was that it fell to 90% which indicates that the noise floor at least is not shot noise limited and is probably both given by the electric noise and the thermal noise. The amplifier after the mixer also adds noise and changes the result.

7.2.2 Equivalent noise.

The noise was also measured with a SRS 510 Lock-In Amplifier. The equivalent bandwidth is 1 Hz corresponding to an integration time of 0.16s (BW=1/ 2πt)(see Fig.17)

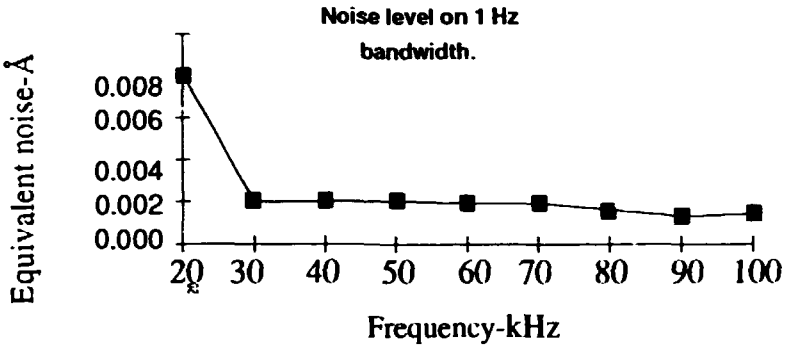

Fig. 17.

If we are dealing with truly white noise then its power is proportional to the bandwidth of the detection system, and its voltage and corresponding displacement is proportional to the square root of the bandwidth. Starting with the mean value of the 1 Hz-noise above 30 kHz; around 0.002 Å, we can calculate what equivalent noise level we ought to have with full bandwidth, 10.7 MHz :

$$\delta_{noise} = \sqrt{BW} \cdot \delta_{1Hznoise} = \sqrt{10.7 \cdot 10^6} \cdot 0.001\text{Å} = 3\,3\text{Å}$$

The 1 Hz-noise level is about 30 times higher than the theoretical limit and 10 times higher than previously measured result. The reason might be that the noise is far from white and the noise density is greater at frequencies below 100 kHz, which is the upper limit for the lock-in amplifier. Another possibility is that the 1 Hz levels are really lower and our results are mostly due to noise and pickup in the Lock-In Amplifier. The starting peak at 20 kHz shows noise from the laser. It is an intensity variation of the laser intensity output coming from the voltage supply. This troublesome noise is seen in fig. 18. The frequency of the noise is 19 kHz and the amplitude is 0.4 % of a maximum total phase shift. This corresponds to 4 Å. A more stable laser source would greatly improve especially the low frequency performances of the interferometer.

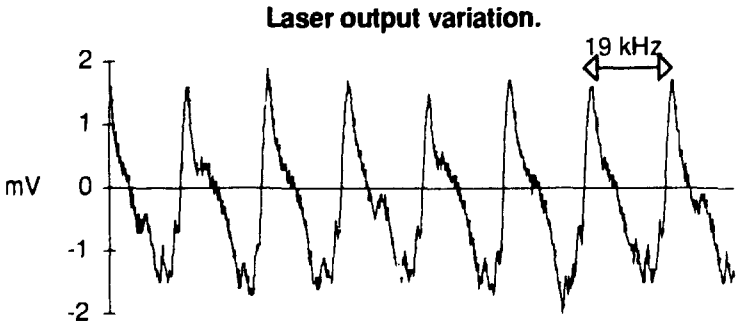

Fig. 18. Laser noise from voltage supply.

7.3 Minimum detectable displacement.

Fig. 19 shows a harmonic mirror displacement at 1 MHz. The output signal is averaged over 256 sweeps, so the noise is severely suppressed. The displacement is 0.35 Å. This is about the limit when averaging the signal, a smaller displacement would hardly be detectable.

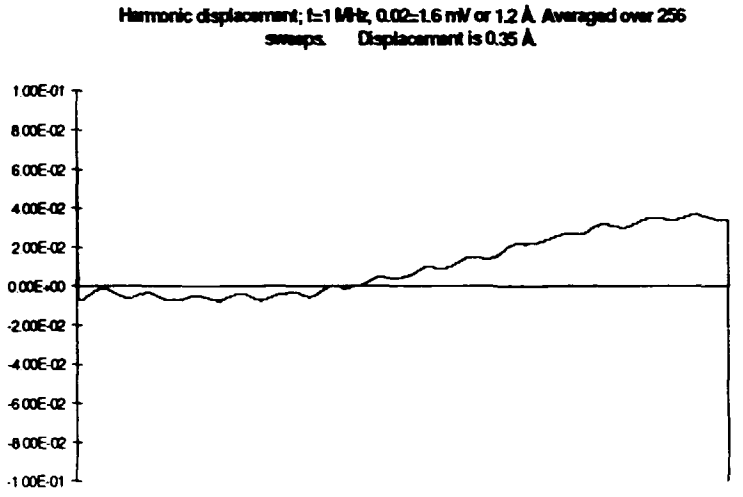

Fig. 19. Minimum detectable displacement, averaged signal.

A measurement without averaging is seen in fig. 20 where the displacement is approx. 0.7 Å. In this picture the signal is approximately as big in amplitude as the noise which was assumed to be the detection limit in Ch. 7.1. 0.7 Å is the value that should be compared with the theoretical value 0.36 Å from Eq. 39.

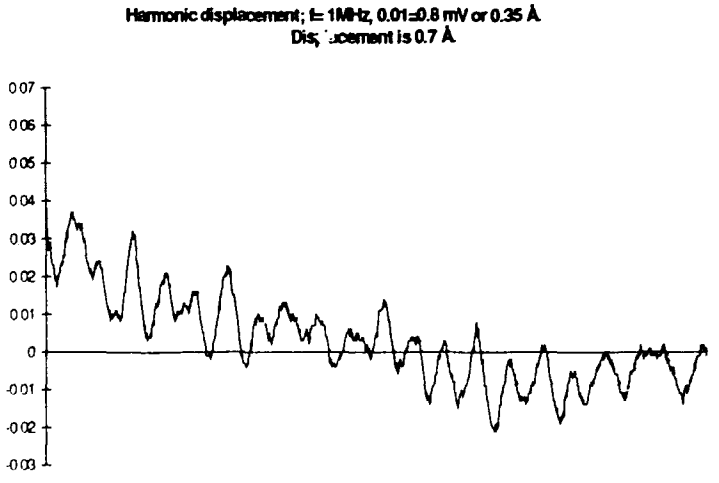

Fig. 20. Minimum detectable displacement, no averaging.

7.4 Accuracy.

Because of the physical nature of the method where the displacement is determined from the relationship between the amplitudes of the displacement phase shift signal and the signal from a phase shift of π the accuracy of the method should be guaranteed. Factors that can change this and distort the result are to be sought in the detection electronics and the way the signal is processed.

Nonlinearities in amplifiers and filters can change the relation between the low frequency calibration signal and the high frequency vibrations. A substantial change in the result has been observed when overloading the amplifier, resulting in a drifting signal to total output (U_{span}) ratio (see Eq. 28).

In the signal processing it is important to trig on the signal when it is close to zero ($\Delta\theta \approx 0$ in Eq. 25). Trigging when $P_m=0.5\beta U_s U_r/R_m$ instead, leads to a maximum error of 18%.

The linearisation in Eq. 15 also demands the displacement amplitude not to exceed 250 Å to stay within an approximation error of 4%.

Averaging the signal may severely lower the detected displacement result due to irregularities in the signal.

8 Improvements.

The idea itself to measure vibrations with interference is very simple; what you need is an interferometer and a detection system. There are many ways to realise these two systems, with their own qualities. The choice of methods in this work is based on studies of articles in the subject, weighted against requirements and resources, plus a lot of trials and errors in the laboratory.
Here I will briefly present a few possible improvements for both the interferometer and the demodulation system.

8.1 Interferometer configuration.

An interesting interferometer set-up can be realised with two beam-splitter and judicious use of the polarisation states (Fig. 21) (Ref. 4).

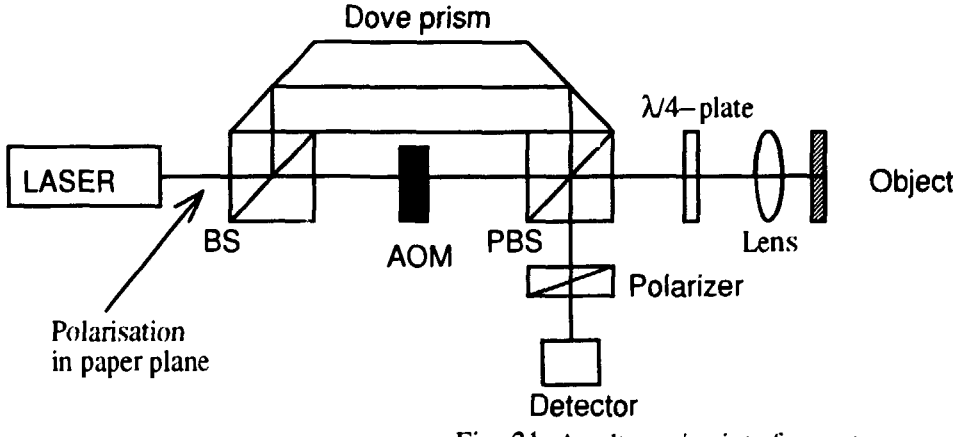

Fig. 21. An alternative interferometer set-up.

This configuration leads to a very compact, mechanically rigid model, that should minimise the environmental influence. A maximum (71%) of the laser power is used for effective interference. The retracing probe beam makes it possible to have different object distances by only moving the lens. When measuring at a distance (within the coherence length) this set-up should be practical. To increase the coherence length and thus the maximum object distance, a single-mode laser should be used.
When using a lens, diffuse object surfaces may be analysed since the lens will both create a well defined measuring point by focusing the beam, and gather the light scattered from a rough surface.
The compactness of this configuration would make it suitable for an easy-to-use mobile system e.g. when mounted on an aluminium profile.

8.2 Detection system.

8.2.1 Improved demodulation.

Eq. 25 gives the output signal from the demodulation system which is the input to the recording module e.g. oscilloscope or transient analyser. The signal includes the variation $\Delta\theta$ due to environment and laser instability. For two reasons this variation is undesirable; first, it shows up as a false vibration and therefore should be erased and secondly it complicates the detection of the true displacement. For small vibrations the phase shifts and thus the signal amplitude will be very small and amplification is desired. Amplification however also affects the $\Delta\theta$ signal in at the same way. When amplifying a displacement signal from 1 mV to 10 mV the $\Delta\theta$ signal of around 500 mV will at the same time increase to 5 V, which requires an oversized and noisy amplifier.
Also because of $\Delta\theta$ the true signal is always detected on the slope of $\Delta\theta$ and especially at lower vibration frequencies the ratio signal to slope can be troublesome.
Fig. 22 shows a detection technique avoiding this problem (Ref 4). Instead of using the AOM-driver signal as reference frequency in the mixer it is extracted from the detector beat signal itself.

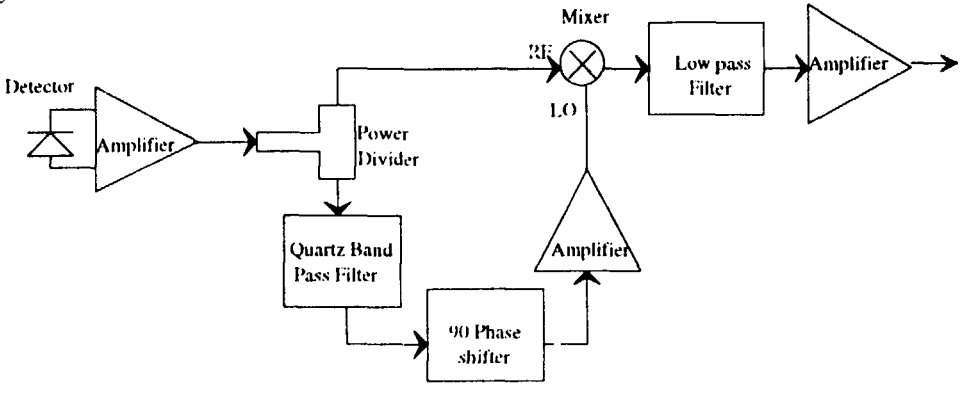

Fig. 22. Demodulation technique avoiding spurious vibrations.

After amplification the detector signal is divided in two parts. One part is fed directly into the mixer. The other part passes trough a very narrow quartz band pass filter centred at 80 MHz the operating frequency of the AOM. The width of the filter may be around 10 kHz which stops high frequency vibrations but lets the low frequency $\Delta\theta$-signal trough. The signal is phase shifted 90 degrees, amplified and is used as reference signal in the mixer. The output signal from the mixer will contain the $\Delta\theta$-signal enclosed in high frequency components (twice the AOM carrier frequency), and the vibration signal without any modulation. The former is stopped by the following filter. The result after the filter and a new amplification is the pure vibration signal limited in frequency by the quartz-filter bandwidth. (See next page).

The mixer output becomes:

$$P_m(t) = \frac{U_{ac} \times U_{ao}}{R_m} =$$

$$2\beta \frac{U_s U_r}{R_m}\left[\cos(2\pi f_{ao}t + \Delta\theta)\sin(2\pi f_{ao}t + \Delta\theta) + \sin(2\pi f_{ao}t + \Delta\theta)\sin(2\pi f_{ao}t + \Delta\theta) \times \Delta\varphi(t)\right] =$$

$$2\beta \frac{U_s U_r}{R_m}\left\{\frac{1}{2}\sin(2\pi 2 f_{ao}t + 2\Delta\theta) + \frac{1 - \cos(2\pi 2 f_{ao}t + 2\Delta\theta)}{2} \cdot \Delta\varphi(t)\right\} =$$

$$\beta \frac{U_s U_r}{R_m}\left\{\sin(2\pi 2 f_{ao}t + 2\Delta\theta) - \cos(2\pi 2 f_{ao}t + 2\Delta\theta) \cdot \Delta\varphi(t) + \Delta\varphi(t)\right\} \qquad (41)$$

Low-pass filter this to get rid of modulation signal :

$$P_{mLP} = \beta \frac{U_s U_r}{R_m} \Delta\varphi(t). \qquad (42)$$

To eliminate variations in optical path, misalignment in the interferometer and slow laser power variations, an automatic gain control (AGC)-amplifier may be used after the detector. The AGC keeps the total signal level constant over time and the need for repetitive calibrations are avoided. The AGC may use a part of the carrier frequency signal as a reference to detect and correct for variations in the output level from the detector. This will also compensate for varying reflectivity of the object surface which otherwise will change the detector output.

8.2.2 PLL-demodulation.

A PLL is a closed loop, feedback system in which an internal oscillator is made to follow the input signal in frequency and phase. The oscillator is a VCO, Voltage Controlled Oscillator and by studying the control voltage on the input to the VCO, we can see how the phase of the PLL input signal fluctuates.

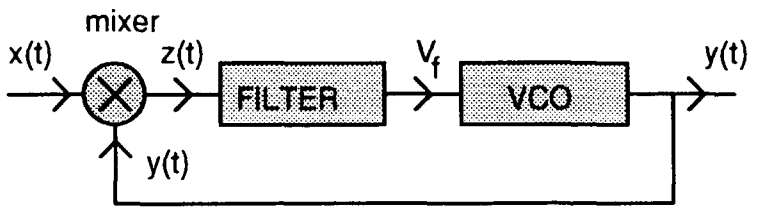

Fig. 23. Phase locked loop (PLL).

If the input signal is :

$$x(t) = A\sin(2\pi f_i t + \theta_i) \tag{43}$$

the output from the VCO, under lock-condition, will be

$$y(t) = B\cos(2\pi f_o t + \theta_o) \tag{44}$$

which is also the feedback input to the mixer. The output from the mixer is :

$$z(t) = \frac{AB}{2}\left\{\sin\left[2\pi(f_i + f_o)t + \theta_i + \theta_o\right] + \sin\left[2\pi(f_i - f_o)t + \theta_i - \theta_o\right]\right\}. \tag{45}$$

The first term is stopped by the low-pass filter and under lock-condition, $f_i = f_o$, and we have :

$$V_f = \frac{AB}{2}\sin(\theta_i - \theta_o). \tag{46}$$

If $(\theta_i - \theta_o) < \frac{\pi}{12}$ and θ_0 is considered a reference phase equalling zero, we end up with :

$$V_f = \frac{AB}{2}\theta_i. \tag{47}$$

The phase $\theta_i = \theta_i(t)$ could be the phase variations induced by the vibrating mirror in a interferometer. The closed loop however has a finite bandwidth, (BW), determined by the loop-filter. If the BW is 50 kHz we can only trace phase shifts below 50 kHz when observing V_f. Faster phase shifts will still be present in the loop though and will show up as an error in the PLL after the mixer.

Thus by observing the output of the mixer z(t) we see the high frequency phase modulation from the mirror displacement.

One advantage with this demodulation technique is that the slow spurious phase-variations from changes in optical path and laser instability are filtered out.
A problem may be to get the PLL to lock on the beat signal. To get an insight in the PLL technique I experimented with a FM receiver. The receiver (based on TAD 7000), basically a PLL, was used to try to demodulate the beat signal from the detector. Even though the VCO's steady-state frequency was correctly tuned, the circuit never locked on the signal. (Ref. 2 and 7).

9 Summary.

A heterodyne laser interferometer for measuring very small vibrations is presented. With the heterodyne interferometry detection technique, where one of the laser beams is frequency modulated with a constant frequency (80 MHz), performance can be improved compared to ordinary homodyne technique. The interference signal has a 80 MHz beat frequency which makes the 1/f-noise very small and the noise level and thus the measuring sensitivity may be limited by thermal or shot-noise.

The beat signal is easy for detection electronics to handle and makes it possible to electronically compensate for influence from environment and laser instability (see Ch.8). The mathematics behind the heterodyne method is described and discussed in Ch. 5 and is followed by examples of both harmonic and transient displacements.

The noise in the output signal sets a limit for the sensitivity of the apparatus and in Ch. 7 this is discussed both theoretically and practically. The theoretical detection limit for the used set-up is 0.36 Å at 10.7 MHz electronic bandwidth while the smallest experimentally detected displacement is 0.7 Å. Ways to lower these limits appears in Ch. 7. The electronic bandwidth of the detection system is also the practical frequency range for detected displacement . In Ch. 8 a few methods of how to improve the apparatus and make it more practical and less influenced by changes in its environment are presented.

Appendix A.

The Acousto-Optic Modulator (AOM).

In the AOM the elasto-optic effect is used; when a material is compressed or stretched its refraction index is changed. An acoustic wave from a piezoelectric transducer creates periodic pressure-variations in a $PbMoO_4$-crystal. These variations result in corresponding variations in stretching and density and thus the refraction index. The relation between the refraction index and the stretching is:

$$\Delta n = -\frac{n_0^3}{2} \cdot p \cdot S$$

where n_0 is the refraction index (unpertubated),

p is the elasteoptic constant, and

S is the streching

In the crystal the refraction index variations acts as a transmission grating for the incident light (see fig.).

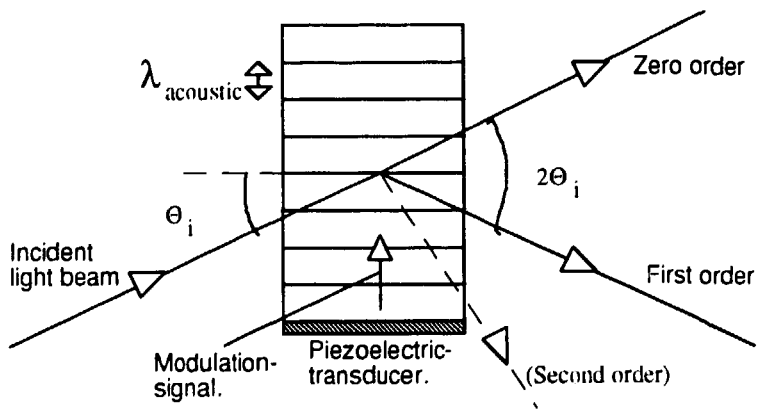

Fig. 24. Acousto optic modulator. Angles are exaggerated.

By varying the amplitude of the RF piezo signal the intensity distribution between the two output beams are controlled. (Ref. 9).

Appendix B.

Mixing of signal when displacement is expressed as a Fourier series.

The mixed signal becomes :

$$P_m(t) = \frac{1}{R_m} U_{ac} \times U_{ao} =$$

$$2\beta \frac{U_s U_r}{R_m} \sin(2\pi f_{ao} t) \left[\cos(2\pi f_{ao} t + \Delta\theta) + \frac{2\pi}{\lambda} \sum_{n=0}^{\infty} d_n \left\{ \sin\left(2\pi (f_{ao} + nf_0)t + \Delta\theta + \varphi_n\right) + \sin\left(2\pi (f_{ao} - nf_0)t + \Delta\theta - \varphi_n\right) \right\} \right] =$$

$$2\beta \frac{U_s U_r}{R_m} \left\{ \frac{1}{2} \sin\left(2\pi f_{ao} t + 2\pi f_{ao} t + \Delta\theta\right) + \frac{1}{2} \sin\left(2\pi f_{ao} t - 2\pi f_{ao} t - \Delta\theta\right) - \right.$$

$$- \frac{2\pi}{\lambda} \sum_{n=0}^{\infty} d_n \left[\frac{1}{2} \cos\left(2\pi (f_{ao} + f_{ao} + nf_0)t + \Delta\theta + \varphi_n\right) - \frac{1}{2} \cos\left(2\pi (f_{ao} - f_{ao} - nf_0)t - \Delta\theta - \varphi_n\right) + \right.$$

$$\left. \left. + \frac{1}{2} \cos\left(2\pi (f_{ao} + f_{ao} - nf_0)t + \Delta\theta - \varphi_n\right) - \frac{1}{2} \cos\left(2\pi (f_{ao} - f_{ao} + nf_0)t - \Delta\theta + \varphi_n\right) \right] \right\} =$$

$$\beta \frac{U_s U_r}{R_m} \left\{ \sin(2\pi 2 f_{ao} t + \Delta\theta) + \sin(-\Delta\theta) - \frac{2\pi}{\lambda} \sum_{n=0}^{\infty} d_n \left[\cos\left(2\pi (2f_{ao} + nf_0)t + \Delta\theta + \varphi_n\right) - \cos(-2\pi n f_0 t - \Delta\theta - \varphi_n) + \right. \right.$$

$$\left. \left. + \cos\left(2\pi (2f_{ao} - nf_0)t + \Delta\theta - \varphi_n\right) - \cos(2\pi n f_0 t - \Delta\theta + \varphi_n) \right] \right\}.$$

Now lowpass filter this :

$$P_{mLP}(t) = \beta \frac{U_s U_r}{R_m} \left\{ -\sin(\Delta\theta) - \frac{2\pi}{\lambda} \sum_{n=0}^{\infty} d_n \left[-\cos(2\pi n f_0 t + \Delta\theta + \varphi_n) - \cos(2\pi n f_0 t - \Delta\theta + \varphi_n) \right] \right\}$$

If P_{mLP} is trigged when $\Delta\theta = 0$ we get

$$P_{mLP}(t) = \beta \frac{U_s U_r}{R_m} \frac{4\pi}{\lambda} \sum_{n=0}^{\infty} d_n \cos(2\pi n f_0 t + \varphi_n)$$

the displacement multiplied by a constant factor.

References.

1 Takahashi, Masuda, Gotoh, and Koyama, Laser Diode Interferometer for Vibration and Sound Pressure Measurements, IEEE Transactions on Instr. & Meas. **38**, 584.

2 Rudd, Ultrasonic non destructive evaluation using laser transducers, Rev. Prog. in Quantitative nondestr. Evaluation, San diego 1982, pg 1763.

3 Ohtsuka, Dynamic measurements of small displacements by laser interferometry, Trans. inst. meas. & Control. **4**, 115. Optics.

4 Lesne, Le Brun, Royer, Dieulesaint, High bandwidth laser heterodyne interferometer to measure transient mechanical displacements, Proc. of the SPIE **863**, 13.

5 Royer, Dieulesaint, Optical detection of sub-angström transient mechanical displacements, IEEE 1986 Ultrasonics Symposium Proc. pg 527.

6 Yariv, Amnon. 1971. Introduction to Optical Electronics. p 254-255.

7 Northrop, Robert B. 1990. Analog Electronic Circuits. pp 364-400.

8 Hecht, Zajac. 1974. Optics.

9 Borgström, Pettersson, Lund LTH. 1990. Optisk Teknik ,compendium. pp [mod (11-13)]

10 Werle, Slemr, Gehrtz, Bräuchle, Wideband noise characteristics ... Applied Optics, Vol. 28, No.9, 1May 1989.